Experimental investigation into the effect of spindle rotational speed on surface roughness and mechanical properties of aluminium 6082T651 welded by friction stir process

M Pita*

Department of Mechanical and Faculty of Engineering and Technology, University of South Africa

ABSTRACT

Selection of the correct parameters during the friction stir welding process is vital. The study entailed an analysis of the mechanical properties and microstructure of aluminium 6082T651 welded by friction stir welding at different spindle rotational speeds (500, 550, 600 and 650 rpm) and constant acceleration of 250 mm/min. Surface roughness of the welded samples was assessed according to ISO 25178. ASTM E384 and ASTM E8/E8M-09 standards were used for hardness and tensile tests respectively. The results show the highest tool rotational speed (650 rpm) to have produced the greatest weld surface roughness, of approximately 19.56 μm. The weldments made by friction stir welding at the highest tool rotational speed of 650 rpm displayed the best mechanical properties.

1. INTRODUCTION

Aluminium alloys are the key structural materials for transport, aerospace, building construction, marine and defence applications [1]. In recent years, lightweight in automotive design and manufacture has come to be one of the most important strategies to meet the growing demands for energy saving, emissions reduction and improved fuel efficiency [2]. Aluminium amalgams are attracting considerable interest around the world as a result of their low thickness, high quality to weight ratio, heat conductivity and erosion resistance [3]. Among novel welding processes, FSW has received widespread attention in various industries, including the automotive industry, for joining steel and aluminum alloys [4]. FSW is a solid-state welding process invented by The Welding Institute (TWI) and has numerous advantages over conventional welding processes [5]. FSW has the capability of fabricating steel joints with excellent toughness and strength, and to perform high-efficiency weldments as compared with fusion welding [6]. The welding process is promoted by the rotation and translation of an axis-symmetric non-consumable tool along the weld centerline [7]. This process is advantageous because it results in sound welds and avoids complications such as cracking, which is associated with fusion welding techniques [8]. It is anticipated that the temperature will increase during an FSW process until it is practically at the material's melting point. [9]. The rotational movement of the tool during FSW causes heat generation which results in localized deformation of the cross-section of the joint section [10]. The tool is plunged into the materials and makes local changes in the stirred zone due to both mechanical deformation and frictional heat [11]. The rotating tool has two major functions: (i) heat

*Corresponding Author: pitam@unisa.ac.za

generation for softening, and (ii) stirring and movement of the materials to be joined. As a consequence of the tool rotation and translation, material travels along the pin to the back of the pin [12]. The severe plastic deformation and high temperature exposure within the stirred zone during FSW result in dynamic recrystallization (DRX) and microstructure evolution, which determine the final grain structure and the performance of weld joints [13]. The friction stir welding technique offers advantages, but it also has drawbacks that make it less effective to use, such as leaving a keyhole after removing the welding tool after each welding process [14]. It is evident that FSW tool controls the amount of material stirred and frictional heat. Therefore, geometry of pin and shoulder are deciding factor to attain good quality welds [15].

Several researchers have conducted studies on tool rotational speed during FSW. The effect of tool travel and rotation speeds on weld zone defects and joint strength of aluminum steel lap joints made by FSW was investigated by Movahedi, Kokabi, Reihani and Najafi, who reported that raising the tool rotation speed enhanced the joint strength slightly [16]. Rezaei, Mirbeik and Bisadi investigated the effect of rotational speeds on the microstructure and mechanical properties of friction stir-welded 7075-T6 aluminum alloy and found that the average grain size of nugget increased from 6.8 to 8.9 mm with increasing rotary speed from 600 to 1550 r/min [17]. A study of the effect of tool rotational speed on the microstructure and mechanical properties of bobbin tool friction stir welded 6082-T6 aluminum alloy was conducted in 2019 by Li and Gong, who reported that when the rotational speed increases, the hardness of the heat-affected zone decreases gradually, and the hardness of the stirred zone increases [18]. From the study of effect of rotational speed on microstructure and mechanical properties of friction stir welded 2205 duplex stainless steel, it was found that the lower rotation speed corresponds to lower heat input during FSW, which resulted in finer recrystallized grains within the stirred zone and thermomechanical affected zone [19]. The tool serves three primary functions; the heating of the workpiece, the movement of material to produce the joint, and the containment of the hot metal beneath the tool shoulder [20]. It was found that the required metallurgical bonding of joints is dependent on the material flow and intermingling level [21]. In general tool rotational speed is considered as one of the most important influential parameters in varying or controlling the mechanical and microscopic properties [22].

Selection of the correct parameters, such as tool rotational speed, during FSW is vital. Incorrect selection of parameters when joining aluminum sheets by means of this technique will have a negative impact on the mechanical properties. The objective of the study was to identify the correct spindle rotational speed to match the welding acceleration of 250 m/s.

2. MATERIAL

The material used in the study was aluminum 6082T651 of a thickness of 6 mm, a width of 75 mm and a length of 200 mm. The chemical composition of the material which was obtained after an EDX spot check is presented in table 1. The welding experiments were conducted at different spindle speeds and at constant acceleration. The spindle rotational speeds are presented in table 2.

Table 1: Chemical composition

Element (Wt %)	Si	Fe	Cu	Mn	Mg	Cr	Zn	Al
Base	1.02	0.306	0.246	0.6	0.74	0.016	0.004	97

Table 2: Spindle rotational speeds

Sample number	Spindle rotational speed (rpm)	Acceleration (mm/min)
Sample 1	500	250
Sample 2	550	250
Sample 3	600	250
Sample 4	650	250

3. METHODOLOGY

3.1. Friction stir welding experiment

The experiments were performed at room temperature using an I-STIR PaR System Technology FSW machine. A cylindrical welding spindle of 20 mm diameter with a conical threaded pin 5 mm in diameter and 5 mm in length was used in the study. During the experiment, the spindle was operated at an angle of 0˚and rotated in a clockwise direction. Single pass welding was used to fabricate the joints for four different spindle rotational speeds, namely 500, 550, 600 and 650 rpm, while the welding acceleration of 250 mm/min was kept constant. The samples to be welded were clamped at six different positions to ensure that they did not separate during the welding process, as shown in figure 1.

Figure 1: Material clamping

3.2. Surface roughness measurement method

A ZEISS LSM 900, illustrated in figure 2, was used for surface topography measurements of the welded samples. During the investigation, the measuring system was controlled by Zen 3.1 software and the surface analysis was carried out using Confomap 8.1 software. The basic details of the measurement were set as follows: image size of 1894 x 1894 pixels, Z-stack 16 slices (310.15 µm), scaling 2496 x 2496 x 54010 µm. All measurements were carried out under identical conditions as these related to, for instance, temperature and lighting. The position of the extracted areas 4.73 mm × 4.73 mm was set to cover the entire width of the sample. The distance of the beginning of the area from the edge of the sample was established at 8 mm (samples welded at 500 and 650 rpm) and 2.5 mm (samples welded at 550 and 600 rpm). ISO 25178 – roughness (S-L) was followed.

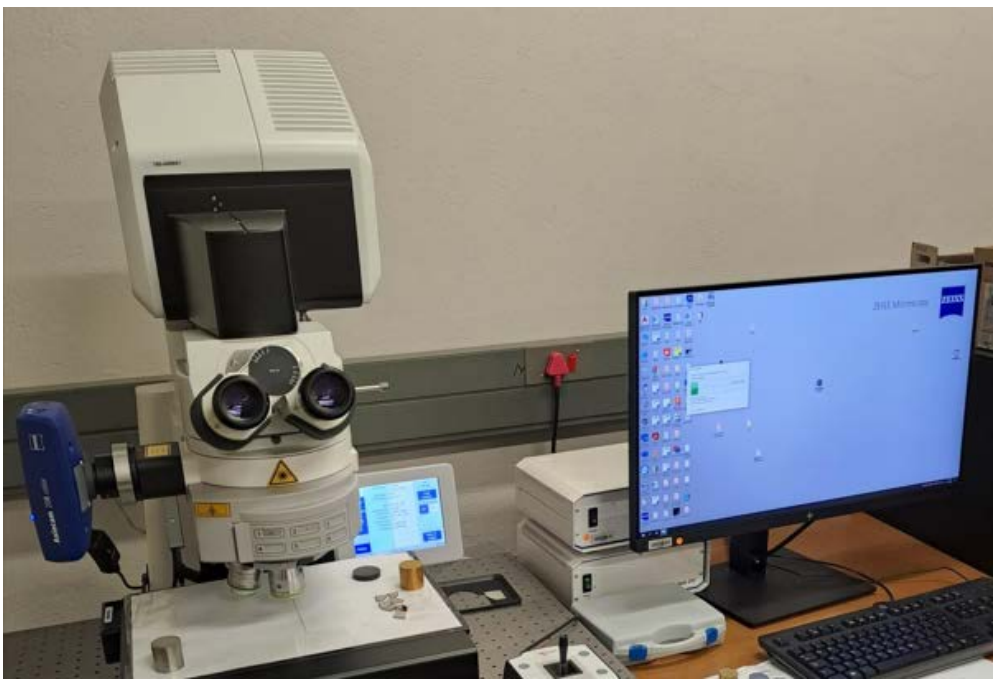

Figure 2: Confocal microscope

3.3. Hardness test method

A hardness test was performed on the weld zone, and lines were drawn at 20 mm intervals from zero to 140 mm, as shown in figure 3. The ASTM E384 standard approach was followed and an EMCO test machine was used. For statistical purposes, eight indentations were constructed. The force was 50 kgf, and the hold time was 30 seconds. The results of the tests were recorded and are presented in table 3.

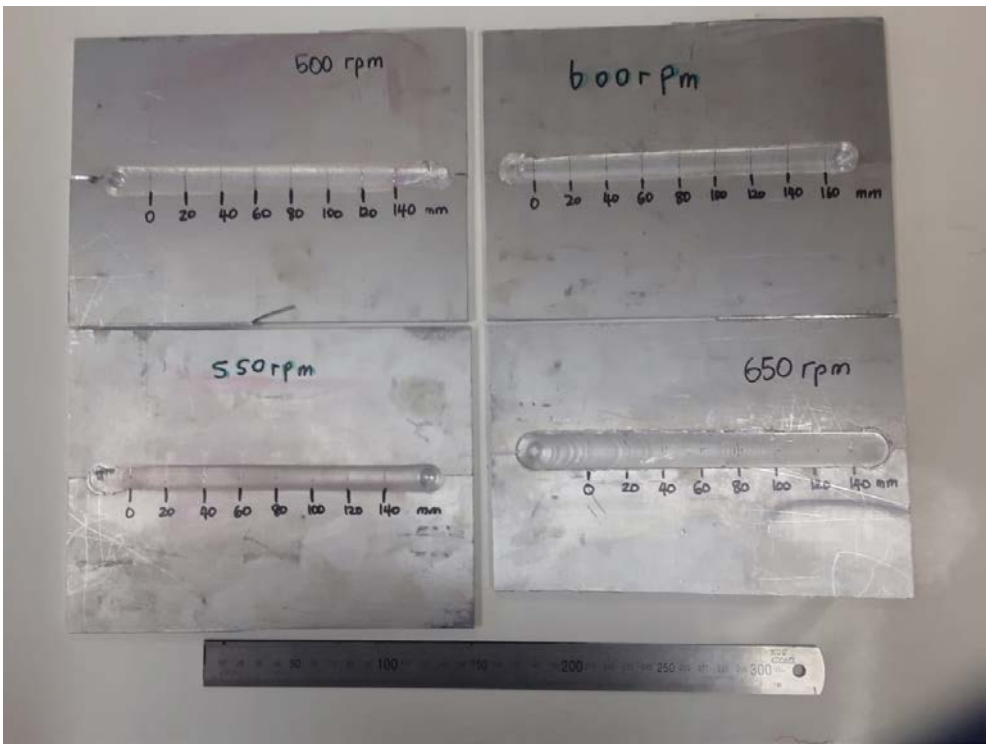

Figure 3: Hardness test positions

Table 3: Average Vickers hardness tests results.

Spindle rotational speed (rpm)	Hardness (50 HV)
500	51.3
550	51.2
600	52.3
650	56.2

3.4. Tensile test method

Three tensile test specimens (illustrated in figure 4) were machine for material welded at tool speeds of 500 and 650 rpm using a water jet. The tests were performed at room temperature according to the ASTM E8/E8M-09 standard using an Instron electro-mechanical machine loaded at a crosshead velocity of 2 mm/minute. The specimens were finally fractured after necking. Tensile stress and displacement results were recorded, and are graphically presented in figure 9.

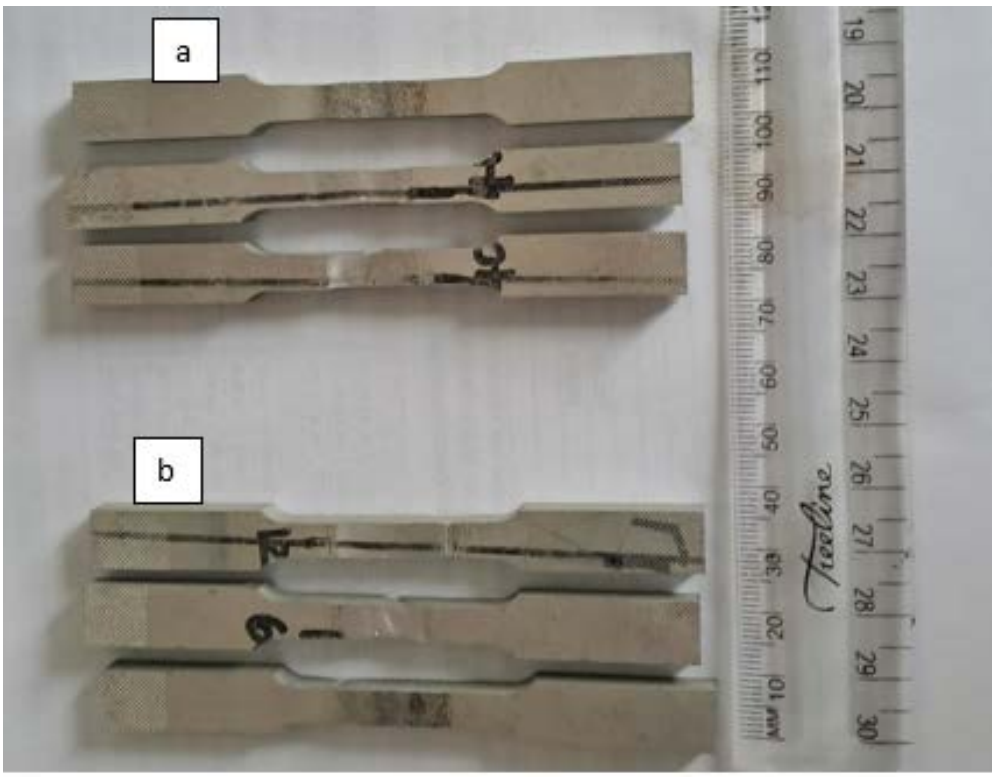

Figure 4: Tensile specimens (a) Sample welded at 500 rpm (b) Sample welded at 650 rpm

4. RESULTS AND DISCUSSION

4.1. Surface roughness

The surface roughness results obtained from the confocal microscopy are presented in table 4 and figures 5 to 7.

From the results presented in table 4, the greatest surface roughness was associated with the fastest speed (650 rpm) and was reported to be 19.56 µm. This was followed by the sample welded at 500 rpm, for which a roughness of 12. 90 µm was measured. As the result of high surface roughness, the surface area had to be increased from 4 mm to 8 mm so as to have the calculated results fall within the limits, as illustrated in figure 5 (a–d). The smoothest welded surface was observed at a tool speed of 550 rpm and was recorded as 3.457 µm, or 82.3%. The highest median value of the Sz parameter of 306.0 µm was obtained at the lowest spindle rotational speed, which was 500 rpm. This was attributed to the fact that the tool accelerated at 250 m/s, which may not be the correct velocity for this tool rotational speed. The speed of 550 rpm gave lower and better results by 242.50 µm (Sz = 63.50 µm). From the same table, the highest height, represented by Sp, was noted in the sample welded with the lowest spindle speed, and was reported as 175.6 µm. The lowest height, 39.79 µm, was obtained at 600 rpm. The highest valley, represented by Sv, was obtained at the lowest tool speed, and was recorded as 130.4 µm. The lowest valley was reported to be 18.81 µm, and was noted at the tool

rotational speed of 550 rpm. The highest mean depth of furrow, 28.68 µm, was obtained at the speed of 650 rpm at the mean density of 656.6 cm/cm^2 and is presented in figure 6d. The lowest mean depth of furrow, 6.355 µm, was noted at 550 rpm with a mean density of 773 µm (figure 6b). It is believed that the key factors in determining the weld quality are sufficient heat input and proper mixing of the plasticized material. When the tool rotational speed is increased, the heat is greater; thus, sufficient plasticizing and mixing results in the formation of a non-defective weld seam [23]. The surface texture and directions are presented in figure 7 (a–d), and isotropy and directional properties of surface features are shown in table 5.

Table 4: Roughness results

Roughness (S-L)	**Sample 500 rpm**	**Sample 550 rpm**	**Sample 600 rpm**	**Sample 650 rpm**
Sq	12.90 µm	3.457 µm	7.552 µm	19.56 µm
Ssk	1.121 µm	0.4385 µm	-1.61 µm	0.02043 µm
SKu	7.680 µm	3.334 µm	11.55 µm	3.729 µm
Sp	175.6 µm	44.69 µm	39.79 µm	88.38 µm
Sv	130.4 µm	18.81 µm	58.39 µm	82.47 µm
Sz	306.0 µm	63.50 µm	98.19 µm	170.9 µm
Sa	9.436 µm	2.753 µm	4.710 µm	14.97 µm
S – filter (λs): Gaussian	0.8 µm	0.8 µm	0.8 µm	0.8 µm
L – filter (λs): Gaussian	8 mm	2.5 mm	2.5 mm	8 mm

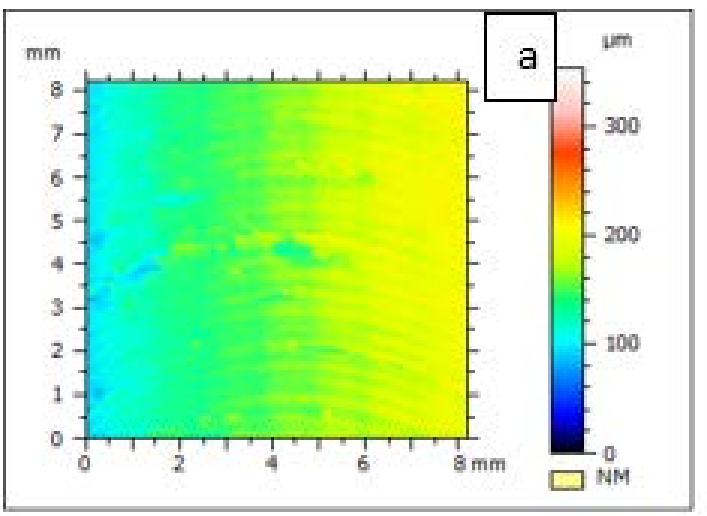

(a)

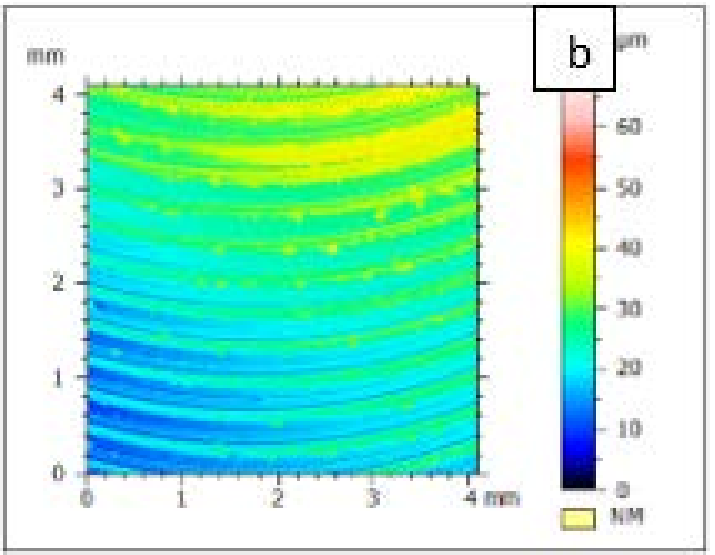
b
mm
μm
4
3
2
1
0
0
1
2
3
4 mm
60
50
40
30
20
10
0
NM

(b)

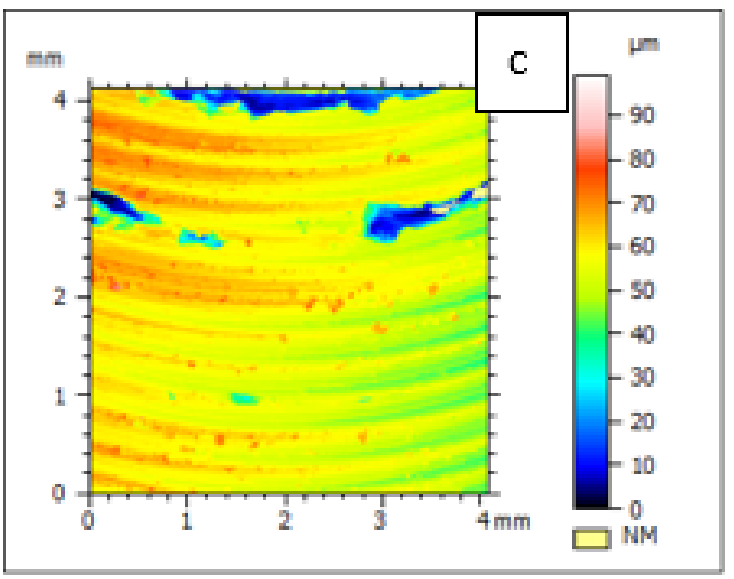
c
mm
μm
4
3
2
1
0
0
1
2
3
4mm
90
80
70
60
50
40
30
20
10
0
NM

(c)

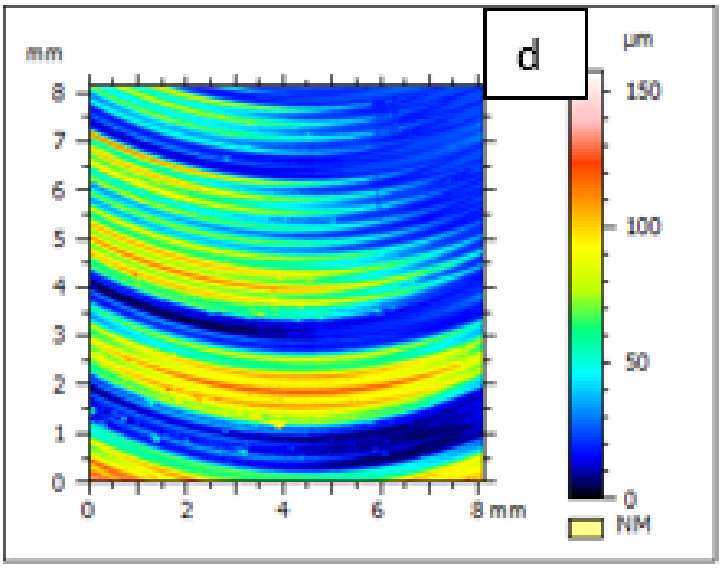

(d)

Figure 5: Surface area (a) Sample 500 rpm (b) Sample 550 rpm (c) Sample 600 rpm (d) Sample 650 rpm

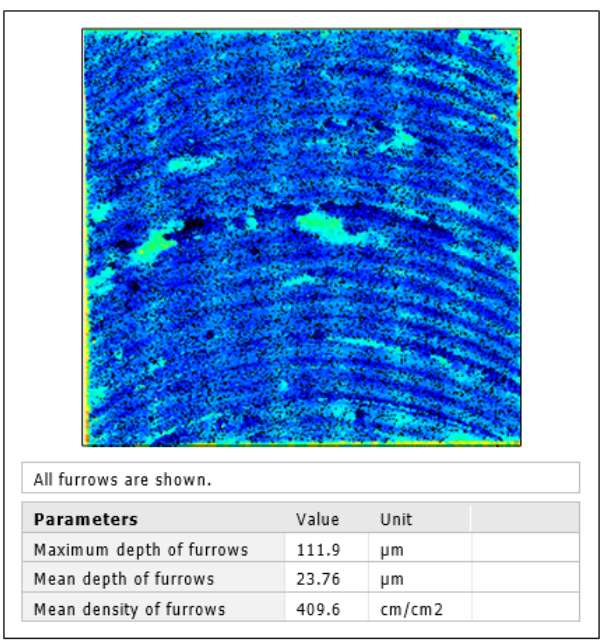

All furrows are shown.

Parameters	Value	Unit
Maximum depth of furrows	111.9	µm
Mean depth of furrows	23.76	µm
Mean density of furrows	409.6	cm/cm2

(a)

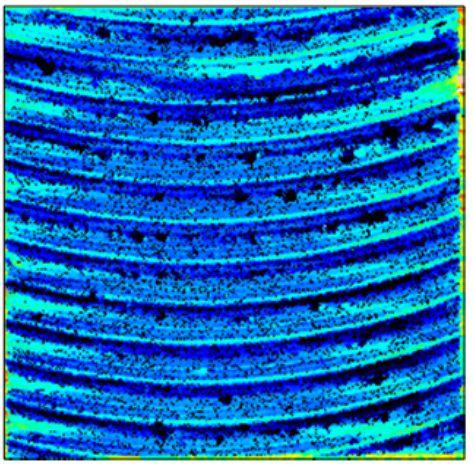

All furrows are shown.

Parameters	Value	Unit
Maximum depth of furrows	35.57	µm
Mean depth of furrows	6.355	µm
Mean density of furrows	773.0	cm/cm2

(b)

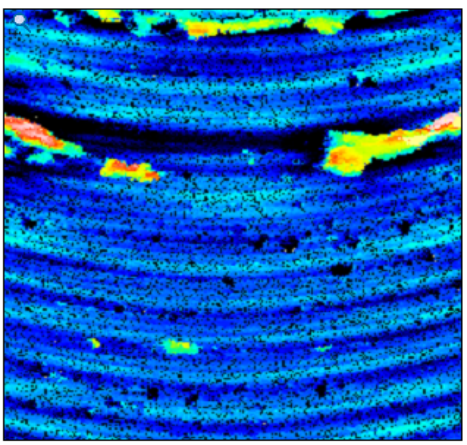

All furrows are shown.

Parameters	Value	Unit
Maximum depth of furrows	59.24	µm
Mean depth of furrows	10.25	µm
Mean density of furrows	770.2	cm/cm2

(c)

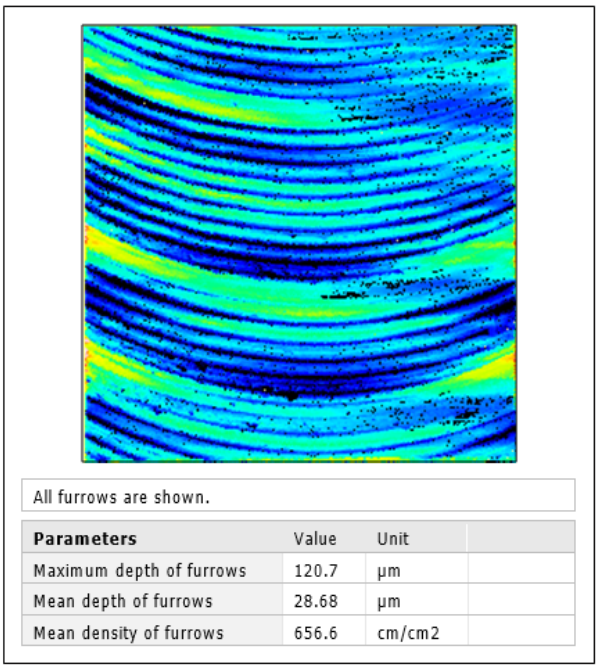

All furrows are shown.

Parameters	Value	Unit
Maximum depth of furrows	120.7	µm
Mean depth of furrows	28.68	µm
Mean density of furrows	656.6	cm/cm2

(d)

Figure 6: Furrows (a) Sample 500 rpm (b) Sample 550 rpm (c) Sample 600 rpm (d) Sample 650 rpm

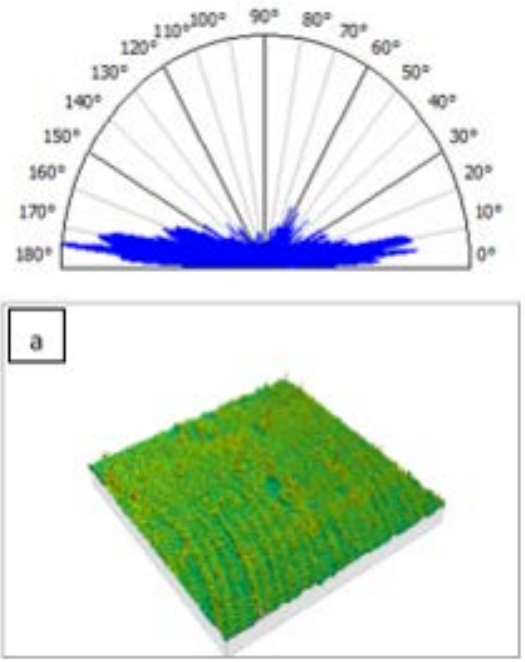

(a)

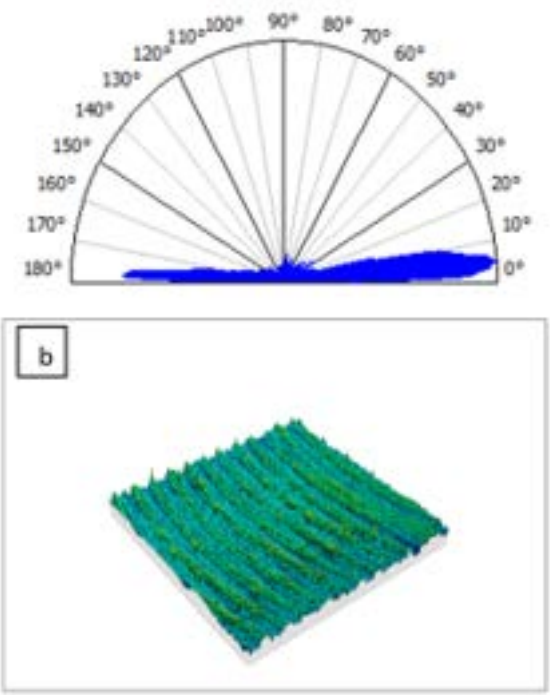
90°
80°
70°
60°
50°
40°
30°
20°
10°
0°
100°
110°
120°
130°
140°
150°
160°
170°
180°
b

(b)

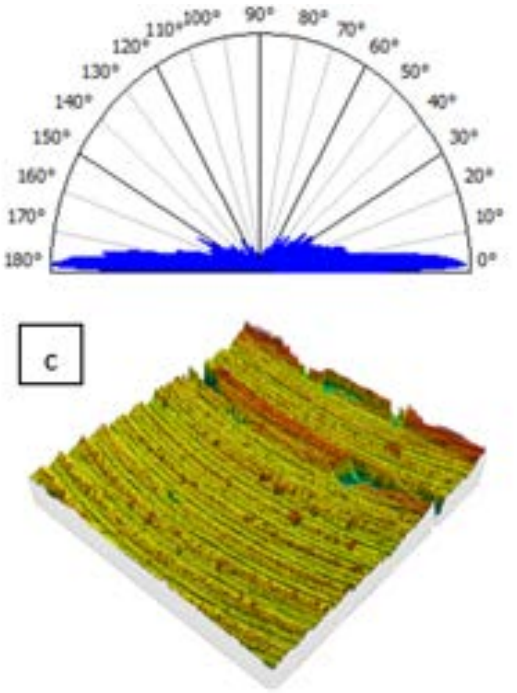
90°
80°
70°
60°
50°
40°
30°
20°
10°
0°
100°
110°
120°
130°
140°
150°
160°
170°
180°
c

(c)

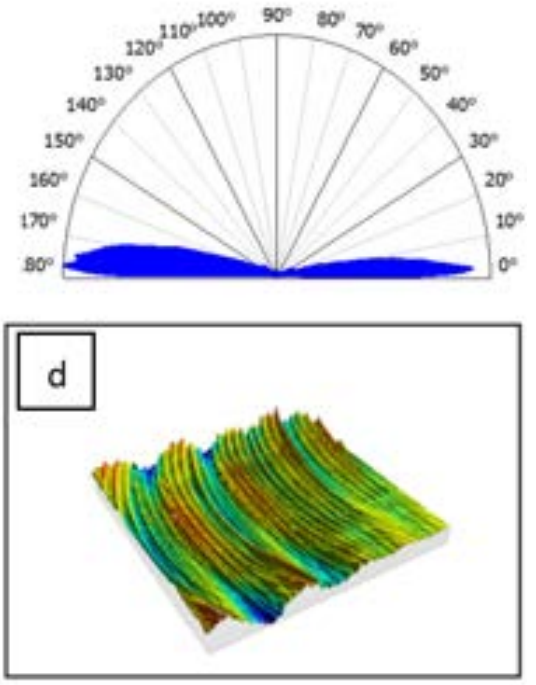

(d)

Figure 7: Surface texture views (a) Sample 500 rpm (b) Sample 550 rpm (c) Sample 600 rpm (d) Sample 650 rpm

Table 5: Isotropy and directional properties of surface features

	Sample (500 rpm)	**Sample (550 rpm)**	**Sample (600 rpm)**	**Sample (650 rpm)**
Isotropy (%)	47.9	15	26.6	27
1st direction (°)	174.3	5	178	177
2nd direction (°)	5.8	178	2	2.5
3rd direction (°)	11	13	14	157

The direction of the texture grooves in the tested samples were similar at different spindle rotational speeds. (The texture grooves are more visible in figures 7b and 7d, where the tool rotational speeds were 550 and 650 rpm respectively.) On the sample (550 rpm), the direction of the texture grooves angle was 5° at the first direction, 178° at the second direction and 13° at the third direction for isotropy of 15.03% (figure 7b). Figure 6d shows a texture groove angle of 177° at the first direction, 2.5° at the second direction, 156.8° at the third direction for isotropy of 27°. The isotropy and directional properties of the surface features are presented in table 5.

4.2. Vickers hardness test

The Vickers hardness test was conducted on the welded zones, and the results are presented graphically in figure 8. The weld hardness was noted as being the same at 500 and

550 rpm. The results show that the weld joint becomes harder as the tool rotational speed increases. At a rotational speed of 650 rpm, the welding hardness was reported to be 56.2 HV, which is 9% greater than at lower speed. Similar results were obtained by [24] during a study of the effect of tool rotational and transverse speed on friction stir weldability of AISI 430 ferritic stainless steels. The hardness in the stir zone is higher than that of the base metal, and it increases as the tool rotational speed increases. This was reported by [25]. It was reported that as the tool rotational speed increases, the peak temperature during FSW becomes higher [23]. For defect-free joints of precipitation-hardened aluminium alloys [26].

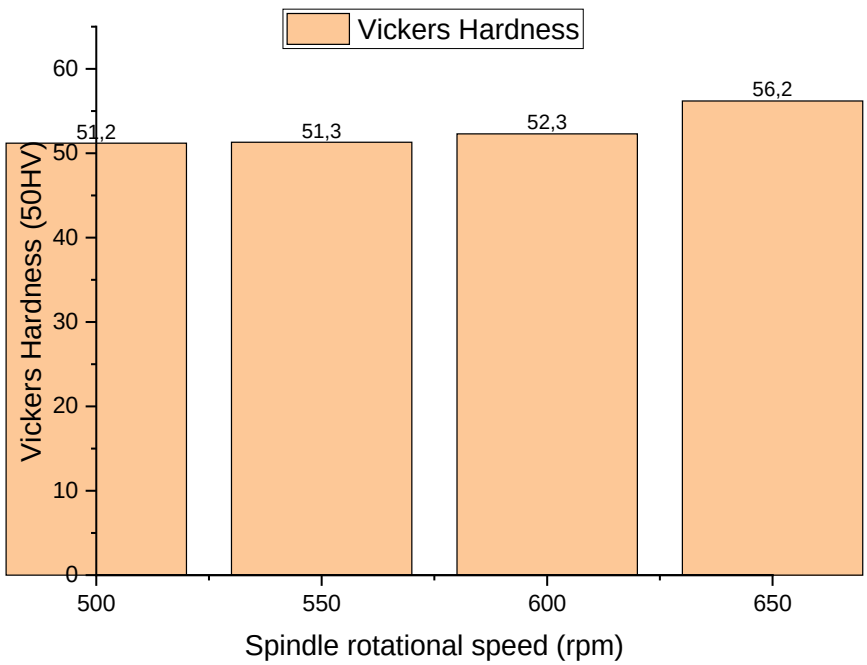

Figure 8: Vickers hardness tests results per spindle rotational speed

4.3. Tensile test results

Three tensile tests per sample were conducted on material welded at 500 and 650 rpm, which were the lowest and highest tool rotational speeds in the study, and the results are illustrated graphically in figure 9 (a–b). The results show that at high tool rotational speed, elevated joint strength was achieved. This indicates that higher tool rotational speed during FSW yields better tensile properties of joint butts. A large increase in welding speed is achieved, with high weld quality and superb joint properties [27]. The rotational speed significantly influences the plastic deformation of the joint, and the tensile deformation of the joint is greater at higher rotational speed [28]. The same results were reported by [29] and [30]. At lower tool rotational speed, there is inadequate heat for the plasticization of the material on the weld zone, and poor adhesion results. The joint strength is reduced by the welding defects.

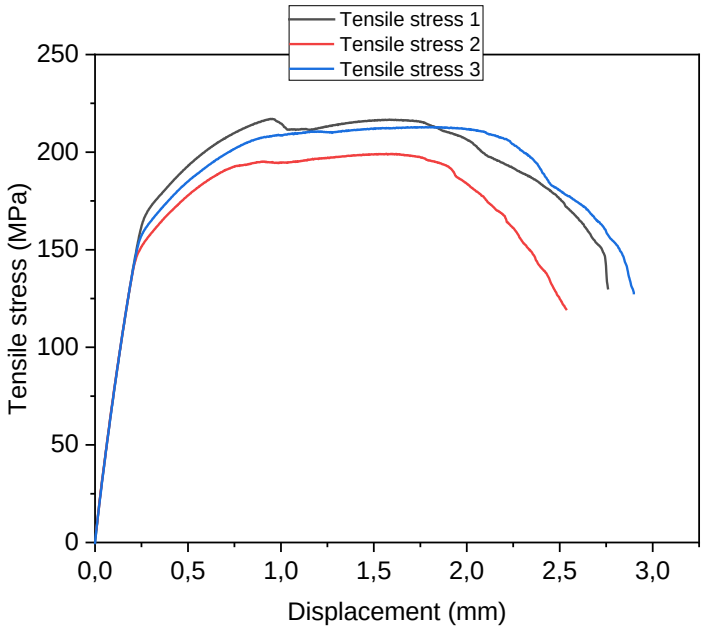

(a)

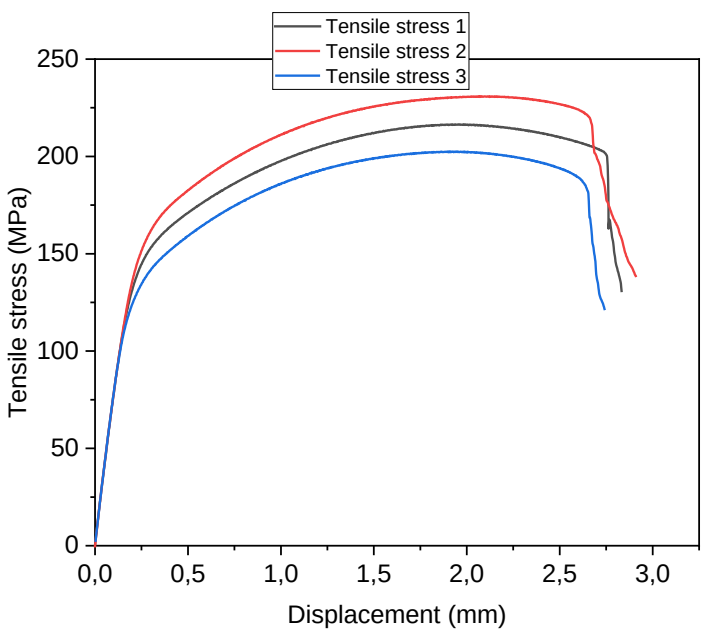

(b)

Figure 9: The relationship between tensile stress and displacement (a) Sample 500 rpm (b) Sample 650 rpm.

5. CONCLUSION

The surface roughness and mechanical properties of aluminium 6082T651 samples welded by FSW were investigated, and the following conclusions drawn. The weld butt made at a tool rotational speed of 650 rpm, which was the highest speed in the study, exhibited the highest surface roughness, of about 19.56 µm. A tool rotational speed of 550 rpm produced a smooth weld. The weldments made by FSW at the highest tool rotational speed of 650 rpm displayed the better mechanical properties. The lower tool rotational speed (500 rpm) does not produce adequate heat to plasticize the material, and this results in poor mechanical properties.

ACKNOWLEDGEMENTS

Mr R Murwamadala and Mr T Gaonnwe are acknowledged for their assistance with the tests. The University of South Africa deserves special recognition for providing the resources and financial assistance necessary to carry out this research.

REFERENCES

[1] W. Muhammad, W. Husain, A. Tauqir, and A. Wadood, “Optimization of Friction Stir Welding Parameters of AA2014-T6 Alloy using Taguchi Statistical Approach,” J. Weld. Join., vol. 38, no. 5, pp. 493–501, 2020.

[2] H.-S. Bang, H.-S. Bang, and K.-H. Kim, “Effects of Process Parameters on Friction Stir Weldability in Dissimilar Joints of AA5052 and Advanced High Strength Steel,” J. Weld. Join., vol. 2232, pp. 1–9, 2021.

[3] S. Nginda and M. Pita, “Investigation of the Mechanical Properties of Aluminum AA4007 Joints Using the MIG and FSW Processes,” in 2022 IEEE 13th International Conference on Mechanical and Intelligent Manufacturing Technologies, ICMIMT 2022, 2022, pp. 11–14.

[4] A. Alimohamady, A. Eghlimi, H. N. Foroshani, M. A. Behzadi, J. Mohammadi, and M. K. Asgarani, “Friction Stir Welding of EN 10130 Low Carbon Steel,” J. Weld. Join., vol. 38, no. 3, pp. 269–277, 2020.

[5] R. Kosturek, L. Śnieżek, J. Torzewski, and M. Wachowski, “Research on the friction stir welding of Sc-modified AA2519 extrusion,” Metals (Basel)., vol. 9, no. 10, pp. 1–15, 2019.

[6] H. H. Abdulkadhum, S. Abdul-Khider, and S. A. Hamza, “Mechanical behavior of friction stir welded high-density polyethylene sheets,” IOP Conf. Ser. Mater. Sci. Eng., vol. 671, no. 1, pp. 1–9, 2020.

[7] S. L. Campanelli, G. Casalino, C. Casavola, and V. Moramarco, “Analysis and comparison of friction stir welding and laser assisted friction stir welding of aluminum alloy,” Materials (Basel)., vol. 6, no. 12, pp. 5923–5941, 2013.

[8] M. Schwartz, “Friction stir welding,” Innov. Mater. Manuf. Fabr. Environ. Saf., no. October, pp. 87–122, 2010.

[9] M. Pita, “Investigation of the effect of tool temperature on microstructure, hardness and wear behaviour of aluminium 6061-T6 alloy welded by the friction stir welding process,” Mater. Des. Process. Commun., vol. 2023, pp. 1–9, 2023.

[10] M. Aali, "Investigation of Spindle Rotation Rate Effects on the Mechanical Behavior of Friction Stir Welded Ti 4Al 2V Alloy," J. Weld. Join., vol. 38, no. 1, pp. 81–91, 2020.

[11] Y.-B. Lim and K.-J. Lee, "Microtexture and Microstructural Evolution of Friction Stir Welded AA5052-H32 Joints," J. Weld. Join., vol. 37, no. 2, pp. 35–40, 2019.

[12] P. Dabeer and G. Shinde, "Perspective of Friction Stir Welding Tools," Mater. Today Proc., vol. 5, no. 5, pp. 13166–13176, 2018.

[13] T. Gaonnwe, M. Mashinini, and M. Pita, "The effect of cold rolling on mechanical properties and microstructure of aluminium 6082 T6 joint by friction stir welding process," in MATEC Web of Conferences 370, 03015 (2022), 2022, vol. 03015, pp. 1–14.

[14] Q. Ismael, M. Fathi, and Z. Abid, "Effect of Friction Stir Welding Parameters on Welding Joint Characteristics: A review," SVU-International J. Eng. Sci. Appl., vol. 4, no. 2, pp. 90–97, 2023.

[15] [15] M. Puviyarasan, L. Karthikeyan, C. Gnanavel, and K. Dhineshkumar, "A Critical review on friction stir based processes," in International Conference for Phoenixes on Emerging Current Trends in Engineering and Management (PECTEAM 2018) A, 2018, vol. 142, no. PECTEAM, pp. 258–266.

[16] M. Movahedi, A. H. Kokabi, S. M. Seyed Reihani, and H. Najafi, "Effect of tool travel and rotation speeds on weld zone defects and joint strength of aluminium steel lap joints made by friction stir welding," Sci. Technol. Weld. Join., vol. 17, no. 2, pp. 162–167, 2012.

[17] H. Rezaei, M. H. Mirbeik, and H. Bisadi, "Effect of rotational speeds on microstructure and mechanical properties of friction stir-welded 7075-T6 aluminium alloy," Proc. Inst. Mech. Eng. Part C J. Mech. Eng. Sci., vol. 225, no. 8, pp. 1761–1773, 2011.

[18] Y. Li, D. Sun, and W. Gong, "Effect of tool rotational speed on the microstructure and mechanical properties of bobbin tool friction stir welded 6082-T6 aluminum alloy," Metals (Basel)., vol. 9, no. 8, 2019.

[19] W. Wang, Y. Hu, T. Wu, D. Zhao, and H. Zhao, "Effect of Rotation Speed on Microstructure and Mechanical Properties of Friction-Stir-Welded 2205 Duplex Stainless Steel," Adv. Mater. Sci. Eng., vol. 2020, no. 2020, pp. 1–13, 2020.

[20] E. T. Akinlabi and S. A. Akinlabi, "Effect of Heat Input on the Properties of Dissimilar Friction Stir Welds of Aluminium and Copper," Am. J. Mater. Sci., vol. 2, no. 5, pp. 147–152, 2012.

[21] S. Memon, M. Paidar, S. Mehrez, K. Cooke, O. O. Ojo, and H. M. Lankarani, "Effects of materials positioning and tool rotational speed on metallurgical and mechanical properties of dissimilar modified friction stir clinching of AA5754-O and AA2024-T3 sheets," Results Phys., vol. 22, no. February, pp. 1–20, 2021.

[22] M. Amatullah, M. Jan, M. Farooq, A. S. Zargar, A. Maqbool, and N. Z. Khan, "Effect of tool rotational speed on the friction stir welded aluminum alloys: A review," in Materials Today: Proceedings, 2022, vol. 62, pp. 245–250.

[23] A. Laska, M. Szkodo, P. Cavaliere, and A. Perrone, "Influence of the Tool Rotational Speed on Physical and Chemical Properties of Dissimilar Friction-Stir-Welded AA5083/AA6060 Joints," Metals (Basel)., vol. 12, no. 10, pp. 1–20, 2022.

[24] M. B. Bilgin and C. Meran, “The effect of tool rotational and traverse speed on friction stir weldability of AISI 430 ferritic stainless steels,” Mater. Des., vol. 33, no. 1, pp. 376–383, 2012.

[25] Y. J. Ko, K. J. Lee, and K. H. Baik, “Effect of tool rotational speed on mechanical properties and microstructure of friction stir welding joints within Ti-6Al-4V alloy sheets,” Adv. Mech. Eng., vol. 9, no. 8, pp. 1–7, 2017.

[26] R. Kosturek, J. Torzewski, M. Wachowski, and L. Śnieżek, “Effect of Welding Parameters on Mechanical Properties and Microstructure of Friction Stir Welded AA7075-T651 Aluminum Alloy Butt Joints,” Materials (Basel)., vol. 15, no. 17, pp. 1–15, 2022.

[27] D. Devaiah, K. Kishore, and P. Laxminarayana, “Effect of Welding Speed on Mechanical Properties of Dissimilar Friction Stir Welded AA5083-H321 and AA6061-T6 Aluminum Alloys,” Int. J. Adv. Eng. Res. Sci., vol. 4, no. 3, pp. 22–28, 2017.

[28] H. Zhang, S. Chen, Y. Zhang, X. Chen, Z. Li, and Z. Yang, “Effect of high rotational-speed friction-stir welding on microstructure and properties of welded joints of 6061-t6 al alloy ultrathin plate,” Materials (Basel)., vol. 14, no. 20, pp. 1–16, 2021.

[29] S. Celik and R. Cakir, “Effect of friction stir welding parameters on the mechanical and microstructure properties of the Al-Cu butt joint,” Metals (Basel)., vol. 6, no. 6, pp. 1–15, 2016.

[30] Sameer, A. Devaraju, S. Gadakary, and S. G, “Effect of Tool Rotational Speeds on Friction Stir Welded AA6082 T6 Aluminium Alloy Joints,” Int. J. Recent Technol. Eng., vol. 9, no. 1, pp. 62–67, 2020.